WAVEGUIDE INVARIANT REVERBERATION MITIGATION FOR ACTIVE SONAR

Ryan Goldhahn, Granger Hickman, Jeffery L. Krolik

Department of Electrical and Computer Engineering
Duke University, Durham, NC 27708-0291

ABSTRACT

Reverberation often limits the performance of active sonar systems. A method of target detection and bottom-feature suppression has been developed exploiting waveguide-invariant phenomena and the frequency-selective fading properties of broadband reverberation in shallow water channels. Specifically, the mean reverberation power is estimated along the striations in the reverberation spectrogram predicted by waveguide invariant theory, where the expected power is constant. Preliminary simulations indicate that significant performance increases are possible over traditional cell-averaging constant false alarm rate (CA-CFAR) methods in the detection of weak targets in reverberation and differentiating between bottom features and water column targets.

***Index Terms*— Clutter, Sonar detection, Sonar signal processing, Waveguide theory, Acoustic scattering**

1. INTRODUCTION

Reverberation often limits the performance of active sonar systems. In particular, backscatter off of a rough ocean floor can obscure target returns and/or large bottom scatterers can be easily confused with water column targets of interest. Moreover, in shallow-water environments, reverberation modeling is exacerbated by multipath propagation and multiple interactions with the bottom. Conventional active sonar detection involves basebanding, matched-filtering, and normalizing the received time series, followed by envelope thresholding. Cell-averaging constant false alarm rate (CA-CFAR) normalization is traditionally used to estimate the threshold above which targets are discriminated against reverberation and noise. In recent years, the use of larger sonar signal bandwidths has been proposed. However, wideband returns have more incoherent reverberation components which often results in higher background variance without a concomitant increase in the target peak due to multipath delay spread. Meanwhile, narrowband signal returns exhibit smaller reverberation-induced variance but exhibit much higher range variability of the mean due to coherent multipath modal interference [1]. Active sonar has thus involved a tradeoff between detection in sub-bands with highly variable mean versus wideband detection in reverberation with larger variance.

In this paper, we present an alternative to CA-CFAR normalization that accounts for the frequency-selective fading characteristics of the multipath channel. The idea is to use the waveguide invariant property [2,3,4] to estimate the frequency-dependent reverberation level at the range cell of interest using neighboring range cells at frequencies along striations in the time-frequency distribution of the sonar return. Bottom scattering and propagation modeling is described below followed by a derivation of the proposed waveguide invariant CFAR detector in Section 3.

2. REVERBERATION MODEL

In shallow-water channels at the frequencies of interest here, normal mode propagation modeling is commonly used [1,5]. Thus consider the Fourier-domain return from two-way propagation to a bottom point scatterer at range, *r,* and complex amplitude, *η(r)*:

$$p(\omega,r) = U(\omega)\sum_{m,n}\phi_m(z_s)\phi_m(z_b)\eta(r)\phi_m(z_b)\phi_n(z_s)\,\frac{\exp\left(-j\left[k_n(\omega)+k_m(\omega)\right]r\right)}{r\sqrt{k_m(\omega)k_n(\omega)}} \tag{1}$$

where ϕ_m are depth-dependent modal eigenfunctions, k_m are modal horizontal wavenumbers, and z_s, z_b, and ω are the source depth, bottom depth, and frequency respectively. The Fourier-domain source waveform is $U(\omega)$. Lumping the depth-dependent terms in *(1)* into coefficients, A_{mn}, the time series from a single point scatterer can be expressed as:

$$x(t,r) = \int_{-\infty}^{\infty} U(\omega)\eta(r)\sum_{m,n}\frac{A_{mn}}{r}\exp\left(-j\left[k_n(\omega)+k_m(\omega)\right]r\right)\exp(j\omega t)\,d\omega \tag{2}$$

A reverberation model can now be synthesized by considering the sum of returns such as *(2)* from a series of independent random scattering centers across range. Thus the scattering amplitude in *(2)* can be replaced by a random zero-mean complex Gaussian white process such that $E\left[\eta(r)\eta^*(r')\right] = \sigma_\eta^2\delta(r-r')$ and summed over range.

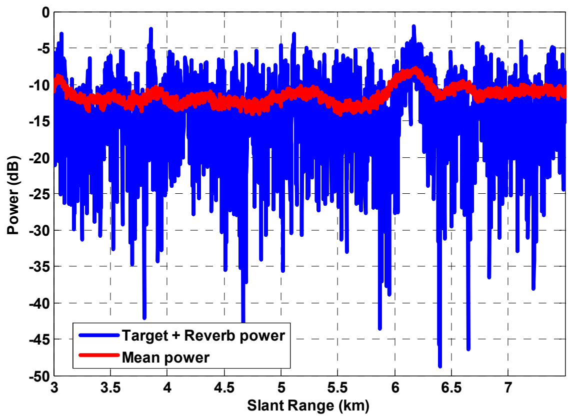

FIG. 1. Simulated reverberation time series of a 400 Hz bandwidth signal. A target is present at 5 km with a SRR of 3 dB. The increase in power at 6.2 km is due to propagation effects.

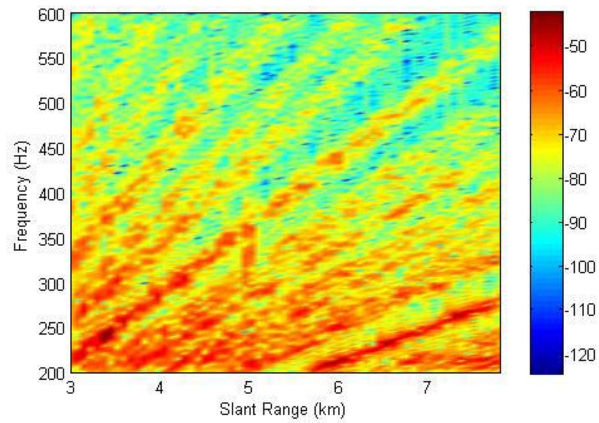

FIG. 2. STFT of a simulated reverberation time series of a 400 Hz bandwidth signal. A target is present at 5 km with a SRR of 3 dB.

An example of the time-domain reverberation return simulated using this model is shown in Figure 1 where the time axis has been converted to slant-range defined by *ct/2.*

An alternative representation of the reverberation data used here consists of taking the short-time Fourier transform (STFT) of time series return. Using a windowing function, *w(t)*, non-zero over an interval *T*, and centered at time τ, the STFT of the reverberation is given by:

$$x(\omega,\tau,T)=\int_0^{\infty}\eta(r)\left(\int_{-\infty}^{\infty} w\left(\frac{t-\tau}{T}\right)x(t,r)\exp(-j\omega t)\,dt\right)dr \quad (3)$$

An example of the STFT magnitude, plotted as a function of time (slant range) and frequency is shown in Figure 2 for the simulated time-domain data in Figure 1.

In this STFT representation, lines of relatively constant reverberation magnitude, known as striations, are clearly evident. This phenomenology has recently been observed in real data collected in the Mediterranean as described in [7]. Note that because a Gaussian model was assumed in the distribution of bottom scatterers, $x(\omega,\tau,T)$ will also be Gaussian-distributed, and Rayleigh-distributed in magnitude. Moreover, although purely time-domain reverberation returns are often modeled as K-distributed [6], because of the inherent windowing used, it is expect that by Central Limit theorem arguments the STFT reverberation data is quite likely to be Rayleigh distributed in practice.

3. CFAR WAVEGUIDE INVARIANT DETECTION

Conventional CA-CFAR detection is performed by comparing the return at each slant range, e.g. in Figure 1, with a threshold estimated by split-window averaging the energy in neighboring range bins [8]. Alternatively, in this paper we consider a CFAR detector based on the STFT of the return, e.g. in Figure 2. Define the test data vector as the STFT coefficients across frequency at the hypothesized target delay, τ_o, $\mathbf{x}=[x(\omega_1,\tau_0,T),\cdots,x(\omega_N,\tau_0,T)]^T$. Detection of the target signal, **s**, in reverberation, **r**, and additive noise, **n**, can then be posed as a binary hypothesis testing problem where:

$$\begin{aligned} \mathrm{H}_0:&\quad \mathbf{x}=\mathbf{r}+\mathbf{n}\sim \mathrm{CN}(0,\mathbf{R}_c) \\ \mathrm{H}_1:&\quad \mathbf{x}=\mathbf{s}+\mathbf{r}+\mathbf{n}\sim \mathrm{CN}(\mathbf{s},\mathbf{R}_c) \end{aligned} \quad (4)$$

In *(4)*, the target return is modeled as an unknown non-random component in complex Gaussian noise with covariance matrix, $\mathbf{R_c}$. Assuming the STFT window, *T*, is longer than the correlation length of the time-series, the STFT coefficients of the reverberation and noise are approximately uncorrelated. Thus, $\mathbf{R_c}$ is a diagonal matrix with non-uniform variances $\sigma_k^2=\sigma^2(\omega_k,\tau_o), k=1,\ldots,N$ along the diagonal.

Assuming for the moment that the $\sigma^2(\omega_k,\tau_o), k=1,\ldots,N$ are known *a priori*, the generalized likelihood ratio test (GLRT) associated with (4) can be written as:

$$\Lambda(\mathbf{x})=\frac{\prod_{i=1}^{N} p(x_i \mid H_1)}{\prod_{i=1}^{N} p(x_i \mid H_0)}=\frac{\max_s\left(\prod_{i=1}^{N}(\pi\sigma_i^2)^{-1}\exp\left(\frac{|x_i-s_i|^2}{\sigma_i^2}\right)\right)}{\prod_{i=1}^{N}(\pi\sigma_i^2)^{-1}\exp\left(\frac{|x_i|^2}{\sigma_i^2}\right)} \quad (5)$$

where s_i and x_i are the i[th] element of ***s*** and ***x*** respectively. Maximizing with respect to **s**, we have $\hat{s}_i=x_i$. Taking the logarithm and simplifying, the GLRT detection statistic

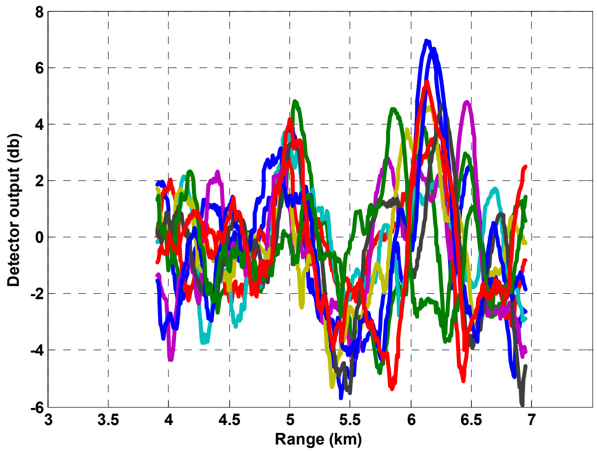

FIG. 3. Realizations of detector output from conventional CA-CFAR processing of a 400 Hz bandwidth signal. A target is present at 5km with a SRR of 3 dB. The target is masked by strong reverberation at 6.2 km.

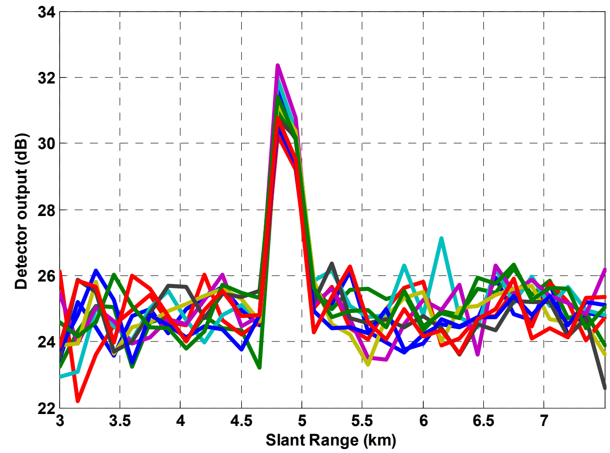

FIG. 4. Realizations of WI detector output of the same signal. The target is clearly visible at 5 km, with the reverberation return at 6 km strongly attenuated.

becomes simply:

$$\ln \Lambda(\mathbf{x}) = \sum_{i=1}^{N} \frac{|x_i|^2}{\sigma_i^2} \tag{6}$$

The GLRT test statistic in *(6)* corresponds to simply normalizing the power in each STFT bin by the reverberation plus noise variance and summing over frequency.

To obtain a CFAR test, however, an estimate of $\boldsymbol{\sigma}_k^2$ in *(6)* is required. The key idea here is to use waveguide invariant theory and associated predictions of the striation pattern in the STFT magnitude to obtain such an estimate. The waveguide invariant [2,3] expresses the frequency-dependence of the horizontal wavenumber differences in a range-independent waveguide in terms of the relationship:

$$k_m(\omega) - k_n(\omega) = \gamma_{mn}\omega^{-1/\beta} \tag{7}$$

where γ_{mn} is a constant determined by mode numbers, and β is the waveguide invariant. Although the exact value of β may fluctuate slightly with mode number difference, it has been shown to remain approximately 1.0 in both simulation and real data for shallow-water waveguides and low order modes [3]. The relation of *(7)* can be applied to the reverberation model of *(3)* by considering the Fourier spectrum of the reverberation return from a clutter patch at delay τ with a time extent T, denoted by $x(\omega,\tau,T)$. Applying *(7)*, after some manipulation it can be shown that:

$$\begin{aligned} E\left[\left|x(\omega,\tau,T)\right|^2\right] &\approx \sigma_\eta^2 \left|U(\omega)\right|^2 \sum_{m,n}\sum_{m',n'} A_{mn}A_{m'n'} \\ &\int_{c(\tau+T/2)/2}^{c(\tau-T/2)/2} \frac{1}{r^2}\exp\left(-j\left[\gamma_{mm'}+\gamma_{nn'}\right]\omega^{-1/\beta} r\right) dr \end{aligned} \tag{8}$$

which yields a relationship between the reverberation level as a function of frequency for a patch in the interval $[\tau - T/2, \tau + T/2]$ and the interval $[\alpha(\tau - T/2), \alpha(\tau + T/2)]$ given by:

$$E\left[\left|x(\omega,\tau,T)\right|^2\right] = \alpha E\left[\left|x\left(\alpha^\beta\omega, \alpha\tau, \alpha T\right)\right|^2\right] \tag{9}$$

where α is a parameter relating one slant range interval to another. Thus the reverberation powers at two ranges are approximately equivalent under the expectation if appropriate changes in frequency are made. The manifestation of *(9)* can be clearly seen in the striations evident in Figure 2.

Since from *(9)* the mean reverberation level in the STFT is approximately constant along the striations, a natural approximately unbiased estimate of $\sigma^2(\omega_k, \tau_o)$ is given by:

$$\hat{\sigma}^2(\omega,\tau) = \frac{1}{N-1}\sum_{\substack{i=1\\ i\neq o}}^{N}\left|x\left(\omega\left(1+\beta\,{}^{\Delta\tau_i}\!/_{\tau}\right), \tau+\Delta\tau_i, T\left(1+{}^{\Delta\tau_i}\!/_{\tau}\right)\right)\right|^2$$

which corresponds to simply averaging along the striations in the reverberation. Placing this estimate in the log-GLRT defined by (6) yields a simple, albeit sub-optimal, CFAR test statistic whose performance will be examined in the following section.

4. RESULTS

To examine the performance of the waveguide invariant (WI) CFAR detector, consider a simulated Pekeris

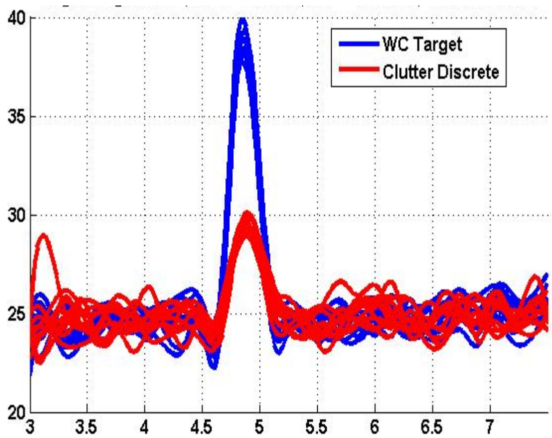

FIG. 5. Realizations of the WI detector output for a 400 Hz bandwidth signal. Cases of a water column target and strong bottom feature at 5 km are examined, each with a SRR of 10 dB. The WI processing suppresses the bottom feature by 10 dB relative to the true target.

waveguide of 100 m in depth with a sound speed of 1500 m/s in the water column and 1800 m/s in the bottom half-space. The transmitter and receiver are located at a depth of 10 m, and the simulated target at 40 m. The frequency band of interest is 200-600 Hz. The environment is assumed to be reverberation-limited, with signal-to-reverberation ratio (SRR) defined as the signal energy to average reverberation power. Simulations were undertaken to compare detection performance between the waveguide invariant-based detector and conventional CA-CFAR detection at various SRR. Cell-average CFAR detection is implemented by split-window normalization of the time-series around the test cell of interest. Shown in Fig. 3 and 4 are several realizations of the output, respectively, of the CA-CFAR and WI detectors at 3 dB SRR. The target is largely obscured in the cell-average CFAR detector, with power at the true target range of 5 km comparable to peaks induced by channel effects (e.g. the false peaks at 6.2 km). In contrast, in the outputs of the waveguide invariant-based detector the target is unambiguously visible at the correct 5 km range and is on average 6 dB higher than the neighboring ranges.

In addition to the problem of target detection against reverberation, the waveguide invariant CFAR detector also shows potential for discriminating between bottom clutter discretes versus water-column scatterers. In Figure 5, the WI detector output is shown for the case of a water-column scatterer versus a bottom scatterer. For both cases, the scatterer was injected at exactly the same SRR of 10 dB in the reverberation time series. In the WI detector output, however, the water-column target is enhanced by approximately 10 dB over the bottom clutter discrete. This behavior is due to the fact that the frequency-selective fading of the clutter discrete is largely normalized out by the reverberation level estimate obtained from neighboring ranges and frequencies.

5. CONCLUSION

Active sonar detection involves a trade-off between detection in sub-bands against highly variable mean reverberation levels versus wider band detection against higher variance reverberation. This work has used the waveguide invariant property to estimate the frequency-selective range-dependent reverberation level at the hypothesized target range. Initial simulation results with a waveguide invariant-based CFAR detector achieved significantly improved normalization of frequency-selective reverberation versus conventional cell-averaged CFAR. Future work will examine ROC performance and more sophisticated CFAR GLRT detectors.

6. ACKNOWLEDGEMENTS

This work was supported by ONR Code 321US under grant N00014-05-1-0023.

7. REFERENCES

[1] K. LePage, "Bottom reverberation in shallow water: Coherent properties as a function of bandwidth, waveguide characteristics and scatterer distributions," J. Acoust. Soc. Am., 106 (6), 3240-3254, 1999.

[2] G. Grachev, "Theory of acoustic field invariants in layered waveguides," Acoust. Phys., 39 (1), 33-35, 1993.

[3] G. D'Spain and W. Kuperman, "Application of waveguide invariants to analysis of spectrograms from shallow water environments that vary in range and azimuth," J. Acoust. Soc. Am., 106 (5), 2454-2468, 1999.

[4] J. Quijano and L. Zurk, "Use of the invariance principle for target tracking in active sonar geometries." OCEANS '06 Boston MTS/IEEE Conference, Sept 18-21 2006.

[5] D. Ellis, "A shallow-water normal-mode reverberation model," J. Acoust. Soc. Am., 97 (5), 2804-2814, 1995.

[6] D. Abraham and A. Lyons, "Novel physical interpretations of K-distributed reverberation," IEEE Journal of Oceanic Engineering, 27, 800-813,2002.

[7] K. LePage et al., "Broad-band time domain modeling of sonar clutter in range dependent waveguides," OCEANS '06 Boston MTS/IEEE Conference, Sept 18-21 2006.

[8] Richards, M., *Fundamentals of Radar Signal Processing*, McGraw-Hill, New York, 2005.